



**Università degli Studi di Genova**  
**Dipartimento di Medicina Sperimentale (DIMES)**  
**PhD Course in Clinical and Experimental Immunology**  
**Cycle XXXVI**

**Coordinator: Prof. Simona Sivori**

**CHARACTERIZATION OF  
MONOCYTE/MACROPHAGE CELL  
POPULATIONS  
IN PERIPHERAL BLOOD  
AND IN THE LUNG TISSUE OF SYSTEMIC  
SCLEROSIS PATIENTS**

**Candidate: Dr. Emanuele Gotelli**

**Tutor: Prof. Maurizio Cutolo**

# INDEX

## Introduction

- Systemic sclerosis - General aspects (pag. 2-5)
- Systemic sclerosis interstitial lung disease (pag. 6-8)
- Systemic sclerosis and monocytes/macrophages (pag. 8-11)

## Aim of the study

(pag. 12)

## Materials and methods

- Sampling from SSc patients and controls (pag. 13)
- Histopathological assessment (pag. 13-15)
- Flow cytometry and gating strategy (pag. 15-18)
- Statistical analysis (pag. 18)
- Ethics statement (pag. 18-19)

## Results

- SSc-ILD and normal lung samples (pag. 20-21)
- Masson's trichrome staining of lung samples (pag. 21-23)
- Immunohistochemistry of lung samples (pag. 23-28)
- SSc patients and flow cytometry of monocytes (pag. 29-33)

## Discussion

(pag. 34-38)

## References

(pag. 39-47)

# INTRODUCTION

## **Systemic sclerosis – General Aspects**

Systemic sclerosis (SSc) is a rare autoimmune connective tissue disease, characterized by microvascular damage, altered activation of innate and adaptive immune response and progressive fibrosis of skin and internal organs [1,2].

The most common clinical and initial manifestation of microcirculatory involvement is Raynaud's phenomenon (RP), present in almost all SSc patients. RP is a paroxysmal vasoconstriction of precapillary arterioles and arteriovenous shunts of hands and feet that causes whitening of the skin (ischemic phase), followed by a bluish (cyanotic phase) and reddish color (erythematous phase) [3]. These repeated episodes of ischemia-reperfusion together with other environmental factors (i.e., viral infections, exposure to intensive cold and/or toxicants) in genetically predisposed subjects generate large amount of reactive oxygen species, that damage endothelial cells and tight junctions.

Therefore, imbalance between increased vasoconstrictor (i.e., involvement of endothelin 1) and decreased vasodilator (i.e., involvement of prostacyclin) peptides reduces the tone of vascular walls with progressive widening [3].

Damaged endothelial cells overexpress adhesion molecules (i.e., ICAM, VCAM) that promote platelets aggregation and innate immune cells

infiltrates, which further increase the permeability and damage of capillaries [4].

Sub-endothelium displays self-antigens that are recognized by antigen-presenting cells, causing the activation of adaptive immunity (T and B lymphocytes).

The concomitant cellular and humoral autoimmune response stimulate the transition of damaged endothelial cells to myofibroblasts (endothelial-to-mesenchymal transition – EndMT), resulting in massive deposition of macromolecules of the extracellular matrix (ECM), in particular type I collagen and fibronectin [5]. Myofibroblasts and altered ECM accumulates in the adventitia and periadventitial of capillaries, promoting a progressive and irreversible fibrosis in the affected skin and internal organs [6].

The evolution of microvascular damage is easily detectable by nailfold videocapillaroscopy (NVC), a safe technique that allows the diameter of skin capillaries to be magnified up to 200 times and to be digitally recorded and analyzed [7].

In course of SSc, the diameter of capillaries (normally less than 20  $\mu\text{m}$ ) progressively dilates until more than 50  $\mu\text{m}$  (giant capillaries). When capillaries break, they release red blood cells metabolized and originate hemosiderin deposits. Then, neoangiogenesis processes are activated to replace the loss of capillaries. In the advanced stages of SSc, neoangiogenic phenomena are insufficient and avascular areas are easily observed with NVC [8].

B lymphocytes produce several autoantibodies in course of SSc that participate in the amplification and perpetuation of the damage [9]. Three major SSc specific autoantibodies are frequently recognized: anti-centromere (ACA), anti-topoisomerase I (anti-Scl-70 - ATA) and anti-RNA polymerase III (RNAP III) [9]. Many additional autoantibodies associated with SSc have also been identified (i.e., anti-fibrillarin, anti-NOR-90, anti-Th/To, anti-RuvBL1/2), although their significance has yet to be clarified [9]. Functional antibodies (i.e. anti-endothelin 1 receptors) have been also found and implicated in the pathophysiology of SSc [10].

The typology of organ involvement is multiple: microvascular (RP, telangiectasias, digital ulcers), cutaneous (skin thickening, puffy hands, sclerodactyly), pulmonary (interstitial lung disease – ILD, pulmonary arterial hypertension – PAH), cardiac (arrhythmias, conduction abnormalities, myocardial disease, pericarditis), renal (isolated proteinuria, isolated decrease in glomerular filtration rate, high intrarenal arterial stiffness, scleroderma renal crisis), gastrointestinal (gastroesophageal reflux disease, lower esophageal sphincter dysfunction, esophageal dysmotility, gastroparesis, gastric antral vascular ectasia, small intestine dysmotility, malabsorption, small intestinal bacterial overgrowth, constipation, intestinal pseudo-obstruction, fecal incontinence) and musculo-skeletal (arthralgias, synovitis, tendon friction rub, myopathy) [2, 11-17]. The frequency of organ involvement is shown in Figure 1.

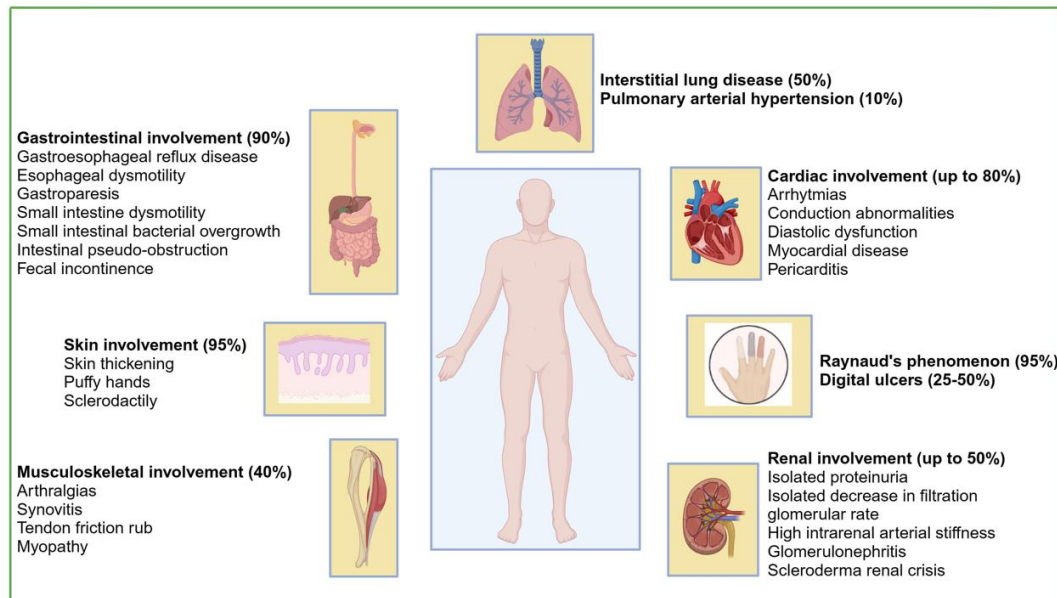


**Figure 1.** Type and frequency of organ involvement in course of systemic sclerosis (original picture created with www.biorender.com).

There are currently no diagnostic criteria for SSc. American College of Rheumatology (ACR) – European Alliance of Associations for Rheumatology (EULAR) 2013 classification criteria are therefore commonly used, with a sensitivity of 91% and a specificity of 92% in classifying a subject as suffering from SSc [18].

These criteria include various disease items and subitems, to which each is assigned a score ranging from 2 to 4. The criteria include skin (thickening of the fingers/fingertip lesions), vascular (presence of RP, abnormal NVC with a SSc-pattern, telangiectasias), pulmonary (PAH and/or ILD) and immunological (scleroderma related antibodies, i.e. ACA, anti-Scl-70, anti-RNAP III) domains. Subjects having a total score of nine or more are classified as having definite SSc [18].

## **Systemic sclerosis interstitial lung disease**

SSc-ILD is defined as pulmonary fibrosis on high resolution computed tomography (HRCT), most pronounced in the basilar portions of the lungs [18,19]. Interstitial abnormalities are reported by HRCT in up to 80% of SSc-patients and half of these cases develop clinically significant SSc-ILD [11].

The pathophysiology of SSc-ILD is multifactorial and involves not only vascular damage with EndMT, but also alveolar damage which activates a local pro-inflammatory innate immune response, with release of interferon gamma (IFN- $\gamma$ ) and interleukin (IL)-6 by dendritic cells and classically activated macrophages M1 [11].

These cytokines further activate T cell response, in particular T helper 2 (T<sub>H</sub>2) lymphocytes. T<sub>H</sub>2 cells produce IL-4, IL-10, IL-13, CCL-18 that stimulate alternatively activation of M2 profibrotic macrophages with production of transforming growth factor  $\beta$  (TGF- $\beta$ ) [11].

TGF- $\beta$  is one of the main drivers of the transition of type II alveolar epithelial cells from an epithelial to a mesenchymal phenotype (epithelial-to-mesenchymal transition – EMT), with a progressive overproduction of ECM components [20].

In synthesis, vascular, alveolar, and immune cell activation contribute to the fibrosis of SSc lung [21].

The clinical manifestations of SSc-ILD are non-specific and patients complain about intolerance to physical exertion, non-productive cough,

atypical chest pain, dyspnea [22]. SSc-ILD patients show often anti-Scl-70 positivity [22].

When SSc-ILD is suspected, pulmonary function tests (PFTs) are a non-invasive method to identify lung involvement [23]. The most characteristic findings are a restrictive ventilatory defect with reduction in lung volumes (forced vital capacity – FVC, and total lung capacity – TLC) and a reduction in the diffusion capacity of carbon monoxide (DLCO) [23].

When these alterations occur, the HRCT of the chest is the gold standard for confirm of diagnosis of SSc-ILD and allows the identification of different radiographic patterns [24]. The most common pattern is non-specific interstitial pneumonia (NSIP), characterized by the presence of ground glass images and with the anatomopathological counterpart of inflammatory or fibrotic lesions in the same evolutive phase, with diffuse or patchy distribution [24].

Less frequent patterns are the usual interstitial pneumonia (UIP) with lesions in different stages up to the honeycomb, organizing pneumonia (OP), lymphoid interstitial pneumonia (LIP) and diffuse alveolar damage (DAD) [25].

Namely, ILD is currently the main cause of death of SSc patients, assuming in some cases a “progressive pulmonary fibrosis” (PPF) phenotype [26-27].

According to the definition proposed by the American Thoracic Society in 2022, PPF is defined “as at least two of the following three criteria occurring within the past year with no alternative explanation: worsening

respiratory symptoms, physiological evidence of disease progression or radiological evidence of disease progression” [27].

Several biomarkers of SSc-ILD have been proposed, such as alveolar epithelial proteins (surfactant proteins A and D, Krebs von den Lungen-6 antigen – KL-6), chemokines and cytokines (CCL2, CCL18, CXCL10), metalloproteinases, acute phase cytokines (i.e., IL-6) up to NVC abnormalities, but their application in daily practice is still limited [28,29].

The treatment of SSc-ILD includes the combined use of immunosuppressive (mycophenolate mofetile, cyclophosphamide, rituximab, tocilizumab) and antifibrotic (tyrosine kinase inhibitor – nintedanib) drugs [30].

### **Systemic sclerosis and monocytes/macrophages**

Monocytes are a subpopulation of leukocytes of myeloid origin [31]. Circulating monocytes can be classified in three different subsets by immunofluorescent flow cytometry, basing on surface expression of CD14 (lipopolysaccharide – LPS – receptor) and CD16 (Fc gamma receptor III):

- Classical: high expression of CD14 and low expression of CD16 (85% of circulating monocytes in healthy subjects)
- Intermediate: expression of both CD14 and CD16 (5% of circulating monocytes in healthy subjects)
- Non-classical: low expression of CD14 and high expression of CD16 (10% of circulating monocytes in healthy subjects) [32].

Monocytes usually extravasate and migrate into damaged tissues where they differentiate into macrophages.

As matter of fact, macrophages are plastic cells that can present a pro-inflammatory (M1) or a pro-fibrotic (M2) phenotype, mainly according to the different cytokine environment [33].

M1 express CD80 and CD86 (co-stimulatory molecules of T lymphocytes) and Toll-like receptor (TLR)-2 and TLR4 on their surface. Their activation stimulates the production of reactive oxygen species and nitric oxide, with pro-inflammatory effects [33].

M2 express CD204 and frequently CD163 (scavenger receptors) as well as CD206 (type I mannose receptor) on the surface and they release IL-4, IL-10 and TGF $\beta$  with an overall anti-inflammatory and profibrotic effect [33].

Depending on the activation stimulus received, M2 macrophages can be further divided into:

- M2a: activated by IL-4 and IL-13 (released by T<sub>H</sub>2 lymphocytes), they produce TGF- $\beta$
- M2b: activated by circulating immune complexes and LPS, they produce IL-10
- M2c: activated by glucocorticoids, they produce IL-10 and metalloproteinases (i.e., matrix metalloproteinase-9)
- M2d: activated by adenosine A2A receptor, they produce vascular endothelial growth factor [34].

In course of SSc, circulating monocytes show a profibrotic phenotype, expressing M2 markers (CD163 and CD204) and producing larger amounts of IL-10 and CCL-18 than healthy controls (HCs) [35,36]. CD14+ circulating monocytes of SSc patients secrete significantly more fibronectin and type I collagen than HCs [37].

Of note, circulating monocytes can express both M1 and M2 markers: in fact, a recent study from our Laboratory demonstrated that CD14+TLR4+CD163+CD204+CD206+ monocytes are significantly more expressed in peripheral blood of SSc patients than HCs and over 40% of these cells also co-expressed CD80 and CD86 (M1 markers) [38]. Circulating CD14+CD80+CD86+TLR4+CD163+CD204+CD206+ cells have been significantly associated with clinically overt SSc-ILD [39].

Macrophages are key regulators of fibrotic processes and are involved in the pathogenesis of SSc-ILD [40]. A droplet-based single-cell RNA-sequencing analysis of SSc-ILD samples revealed a predominant proliferating FABP4, INHBA and SERPING1 (FABP4<sup>hi</sup>) macrophage population, with a significant higher proportion of proliferating macrophages expressing SPP1, CCL2 and MERTK (SPP1<sup>hi</sup>), when compared to HCs [41].

Of note, SPP1<sup>hi</sup> and FABP4<sup>hi</sup> macrophages show an upregulation in type I interferon signaling and production (which enhances the release of further cytokines from macrophages in an autocrine loop) and FABP4<sup>hi</sup> macrophages show an upregulation in IL-6 signaling [42].

Moreover, an epigenetic regulation of SPP1 macrophage differentiation have been identified using a single-cell regulatory network inference and clustering. Several transcription factors are involved in the regulation of chromatin structure of SPP1 macrophages, i.e., microphthalmia-associated transcription factor, sterol regulatory element binding transcription factor 1, Kruppel-like factor 6 [43].

M2 (CD163+, CD206+) subset of macrophages is the most represented in SSc-ILD and release large amount of TGF $\beta$ , that promote EMT and the differentiation of fibroblasts into myofibroblasts [44-46].

In addition to TGF $\beta$ , pulmonary M2 cells in SSc release IL-6, CCL-18 and osteopontin, that stimulates type I collagen production [47]. The increased production of ECM proteins supports the progressive lung fibrotic process [48,49].

## **AIM OF THE STUDY**

The Study was divided into two aims.

The first aim was to characterize the distribution of macrophage phenotypes in lung biopsies of SSc-ILD patients by immunohistochemistry, comparing it with normal lung controls (NLC).

In particular, the different macrophage phenotypes were investigated, to characterize the M1, M2 and/or hybrid M1/M2 populations, in SSc-ILD lung samples.

The second aim was to compare prevalent surface markers observed in SSc-ILD lung tissue macrophages with those of peripheral monocytes of a second cohort of SSc patients by flow cytometry, correlating them with radiographic ILD and anti-Scl-70 positivity.

# **MATERIALS AND METHODS**

## **Sampling from SSc patients and controls**

SSc-ILD lung samples were obtained from SSc patients that underwent lung transplantation for severe ILD between 2005 and 2010 at the University of Pittsburgh Medical Center, Pittsburgh, Pennsylvania (US).

Normal lung controls (NLC) were obtained from non SSc-patients that underwent lung biopsy for diagnostic purposes in 2022 at the IRCCS Ospedale Policlinico San Martino, Genova, Italy. Healthy areas of NLC were identified by the same expert Pathologist.

Peripheral monocytes for flow cytometry analysis were obtained from SSc patients in 2019 at the Division of Clinical Rheumatology, IRCCS Ospedale Policlinico San Martino, Genova, Italy.

All SSc patients met 2013 ACR/EULAR classification criteria for SSc and SSc-ILD was defined as “pulmonary fibrosis on HRCT, most pronounced in the basilar portions of the lungs” [18].

Clinical parameters regarding SSc-lung involvement (ILD at HRCT and PFTs, including values of FVC and DLCO) and concomitant therapy were collected for each SSc patient.

## **Histopathological assessment**

Lung tissues were fixed in 10% formalin and embedded in paraffin. They were cryostat-sectioned to obtain ten serial sections (4 µm thick).

One section was stained with Masson's trichrome staining to identify collagen deposition (blue color) and cells infiltrate (violet color).

Other sections were incubated for single immunostaining with following primary antibodies:

- Mouse anti-human CD68 (pan specific macrophage marker, Clone KP1, Biocare, Pacheco, California, USA) – dilution 1:50
- Mouse anti-human CD80, CD86, TLR4 (M1 markers - Santa Cruz Biotechnology, Dallas, Texas, USA) – dilution 1:50
- Rabbit anti-human CD163 and CD206 (M2 markers - Cell Signaling Technology, Danvers, Massachusetts, USA) – dilution 1:50
- Mouse anti-human CD204 (M2 marker) (cod. sc-166184, Santa Cruz Biotechnology, Dallas, Texas, USA) – dilution 1:50.

Primary antibodies were detected with ready-to-use conjugated secondary antibodies (Biocare).

Histology sections were digitalized using Leica AT2 scanner (Nussloch, Germany). Scans were performed using the fully automated mode (20x and 40x magnification).

Fibrosis of lung samples was visually graded according to Ashcroft criteria:

- 0 = normal lung
- 1 = minimal fibrous thickening of alveolar or bronchiolar walls
- 2 = intermediate grade between 1 and 3
- 3 = moderate thickening of walls without obvious damage to lung architecture
- 4 = intermediate grade between 3 and 5

- 5 = increased fibrosis with definite damage to lung structure and formation of fibrous bands or small fibrous masses
- 6 = intermediate grade between 5 and 7
- 7 = severe distortion of structure and large fibrous areas, including “honeycombing lung”
- 8 = total fibrous obliteration of the field [50].

An automated quantification of lung fibrosis was performed with open-source version of Orbit Image Analysis software (Actelion Pharmaceuticals Ltd, Allschwil, Switzerland). The software provided a semiquantitative analysis, ranging from 0 (absence of fibrosis) to 1 (complete fibrosis) [51].

Cells positive for CD68, CD204, CD206, CD163, TLR4, CD80, CD86 in the alveoli of SSc-ILD lungs were quantified by the Image Scope 12.3 Software (Leica Biosystems, Milan, Italy) [52]. Based on the User’s guide of Image Scope analysis software, a visual representation of the dark-brown colored cells allowed to create a markup image and the appropriate algorithm to analyze the slides and to have a quantitative result of the percentage of positive cells. The alveoli containing CD68+ infiltrates were considered and analyzed for the expression of other surface markers [52].

### **Flow cytometry and gating strategy**

A volume of 3 mL of peripheral blood was collected in a lithium-heparin single tube for each SSc patient.

To define the monocyte/macrophage lineage, the surface markers CD14, CD16 and CD45 were investigated using conjugated primary antibodies

anti-human CD14-FITC (Miltenyi Biotec, Bergisch Gladbach, Germany), CD16-APC AlexaFluor 700 (Beckman Coulter, Brea, California, USA), and CD45-Krome Orande (Beckman Coulter).

To characterize the M1 phenotype of circulating monocytes, the surface markers CD80 and TLR4 were investigated using conjugated primary antibodies anti-human CD80-PEVio700 (Miltenyi Biotec), and TLR4-BV421 (Biolegend, San Diego, California, USA).

To characterize the M2 phenotype of circulating monocytes, CD163, CD204 and CD206 were investigated using conjugated primary antibodies anti-human CD206-PerCPVio700, CD204-PE and CD163-PEVio615 (Miltenyi Biotec).

To exclude the presence of dendritic cells, the surface marker CD1c was investigated using the conjugated primary antibody anti-human CD1c-APC Cy7 (Biolegend, San Diego, California, USA).

Finally, the expression of 6-sulfo LacNAc (Slan) in circulating monocytes was also investigated using the primary antibody anti-human Slan-APC (Miltenyi Biotec).

The Flow Cytometry analysis was performed using Navios Flow Cytometer and the Kaluza analysis software (Beckman Culter), evaluating a total of  $5 \times 10^6$  cells and detecting more than 30 events in the smallest subset investigated, according to consensus guidelines [53].

The gating strategy used in this study started from the detection of the monocyte population characterized as CD45<sup>+</sup>CD14<sup>+</sup>CD16<sup>+</sup>cells in the leukocyte population of SSc patients and HCs (Figure 2).

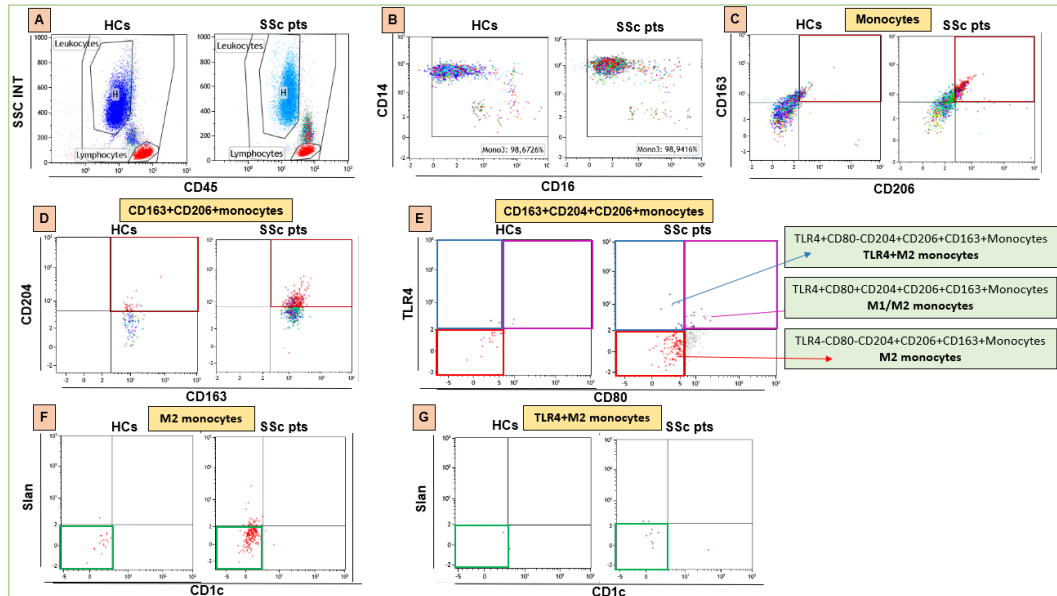


**Figure 2.** Gating strategy for the detection of circulating M2 and TLR4+M2 monocytes in systemic sclerosis patients (SSc pts) and healthy controls (HCs).

**(A)** Representative flow cytometry scatter plot of leukocytes (CD45+cells). **(B)** Representative flow cytometry scatter dot plot of circulating monocytes (CD45+CD14+CD16+cells) in the leucocyte population. Representative flow cytometry scatter dot plot with quadrant regions of **(C)** circulating CD163+CD206+ cells in the monocyte population; **(D)** CD163+CD204+CD206+ monocytes in CD206+CD163+cells; **(E)** TLR4-CD80-CD163+CD204+CD206+ monocytes (M2 monocytes), TLR4+CD80-CD163+CD204+CD206+ monocytes (TLR4+M2 monocytes), TLR4+CD80+CD163+CD204+CD206+ monocytes (M1/M2 monocytes) in the CD163+CD204+CD206+ monocytes; **(F)** Slan-CD1c-M2 monocytes in TLR4-CD80-CD163+CD204+CD206+ monocytes (M2 monocytes) and **(G)** Slan-CD1c-TLR4+M2 monocytes in TLR4+CD80-CD163+CD204+CD206+ monocytes (TLR4+M2 monocytes) of NLC and SSc pts.

In the monocyte population, circulating monocytes expressing M2 phenotype markers and characterized as

CD45<sup>+</sup>CD14<sup>+</sup>CD16<sup>+</sup>CD204<sup>+</sup>CD206<sup>+</sup>CD163<sup>+</sup>TLR4<sup>-</sup>CD80<sup>-</sup>cells (M2 monocytes), circulating M2 monocytes expressing TLR4 (CD45<sup>+</sup>CD14<sup>+</sup>CD16<sup>+</sup>CD204<sup>+</sup>CD206<sup>+</sup>CD163<sup>+</sup>TLR4<sup>+</sup>CD80<sup>-</sup>cells; called TLR4<sup>+</sup>M2 monocytes), and monocytes expressing both M1 and M2 markers (CD45<sup>+</sup>CD14<sup>+</sup>CD16<sup>+</sup>CD204<sup>+</sup>CD206<sup>+</sup>CD163<sup>+</sup>TLR4<sup>+</sup>CD80<sup>+</sup>cells; called mixed M1/M2 monocytes) were also investigated.

### **Statistical analysis**

Statistical analysis was carried out using GraphPad Prism and Datatab® Statistics Calculator. Continuous variables were reported as mean value and standard deviation (SD) or median, when appropriate, categorical variables as count and percentage. For comparing two group values, T-student and Levene test of variance equality have been performed while for groups that did not follow Gaussian distribution, the two-tailed Mann-Whitney U test was used. Spearman's rank correlation was used to calculate the relationship between ordinal variables, whereas Pearson's correlation analysis was used for metrically scaled variables. Any p values equal or lower than 0.05 were considered statistically significant.

### **Ethics statement**

This Project was conducted in accordance with all applicable laws and regulations, including, but not limited to, the International Harmonization Guideline (ICH) for Good Clinical Practice (GCP), European Union guidelines and ethical principles that originate in the Declaration of

Helsinki. Lung samples analyses were carried out in accordance with recommendations of Medical University of South Carolina (Charleston, USA), University of Pittsburgh (Pennsylvania, USA) Institutional Review Boards and IRCCS Ospedale Policlinico San Martino (Genova, Italy) with written informed consent from all the patients.

Flow cytometry study was approved by the Ethics Committee of IRCCS Ospedale Policlinico San Martino, Genova, Italy (273-reg-2015) and all patients signed the informed consent.

## RESULTS

### SSc-ILD and normal lung samples

SSc-ILD lung samples (SSc-71, SSc-72, SSc-73, SSc-74, SSc-77, SSc-83, SSc-88, SSc-90, SSc-91) were obtained from nine SSc-ILD patients (6 females, 3 males, mean age  $50 \pm 9$  years) who underwent lung transplantation for SSc-ILD.

Normal lung samples areas were obtained from five non-SSc patients (2 females, 3 males, mean age  $58 \pm 23$  years) who underwent lung biopsy for diagnostic purposes (two cases of pneumothorax and three cases of lung cancer). Demographic data of patients are resumed in Table I.

	SSc-ILD patients (n=9)	Non-SSc patients (n=5)
Age (years, mean $\pm$ SD)	$50 \pm 9$	$58 \pm 23$
Gender (Female/Male)	6/3	2/3
Ethnicity (Caucasian/Afro-American)	7/2	5/0
Smokers/Non-smokers	2/7	1/4
Pneumothorax/Lung cancer	0/0	2/3
FVC (reference percentage, mean $\pm$ SD)	$39.6 \pm 12.3$	-
FEV1 (reference percentage, mean $\pm$ SD)	$45.5 \pm 14.1$	-
TLC (reference percentage, mean $\pm$ SD)	$37.6 \pm 9.0$	-
DLCO (reference percentage, mean $\pm$ SD)	$17.4 \pm 4.6$	-
Immunosuppressive drugs (mycophenolate mofetil / calcineurin inhibitors / basiliximab / alemtuzumab)	4/4/2/2 (combination therapies)	-
Antifibrotic drugs (nintedanib /pirfenidone)	0/0	-

**Table I.** Demographic data of SSc-ILD patients with respiratory parameters at time of lung transplantation and non-SSc patients. DLCO = Diffusion Lung Carbon Monoxide; FEV1 = Forced Expiratory Volume in the first second; FVC = Forced Vital Capacity; ILD = Interstitial Lung Disease; SD = Standard Deviation; SSc = Systemic sclerosis; TLC = Total Lung Capacity.

### **Masson's trichrome staining of lung samples**

Masson's trichrome staining identified abundant collagen deposition (blue color) and cells infiltrate (violet color) in stroma and alveoli of every SSc-lung samples. Most alveoli were collapsed and occluded by connective tissue and cellular infiltration.

All SSc-ILD lung samples were estimated to have a visual fibrosis grading score higher than 5/8 and the mean of automatic semi-quantification of collagen tissue was  $0.82 \pm 0.12$  ( $p < 0.001$  vs NLC).

Masson's trichrome staining of all SSc-ILD samples is reported in Figure 3.

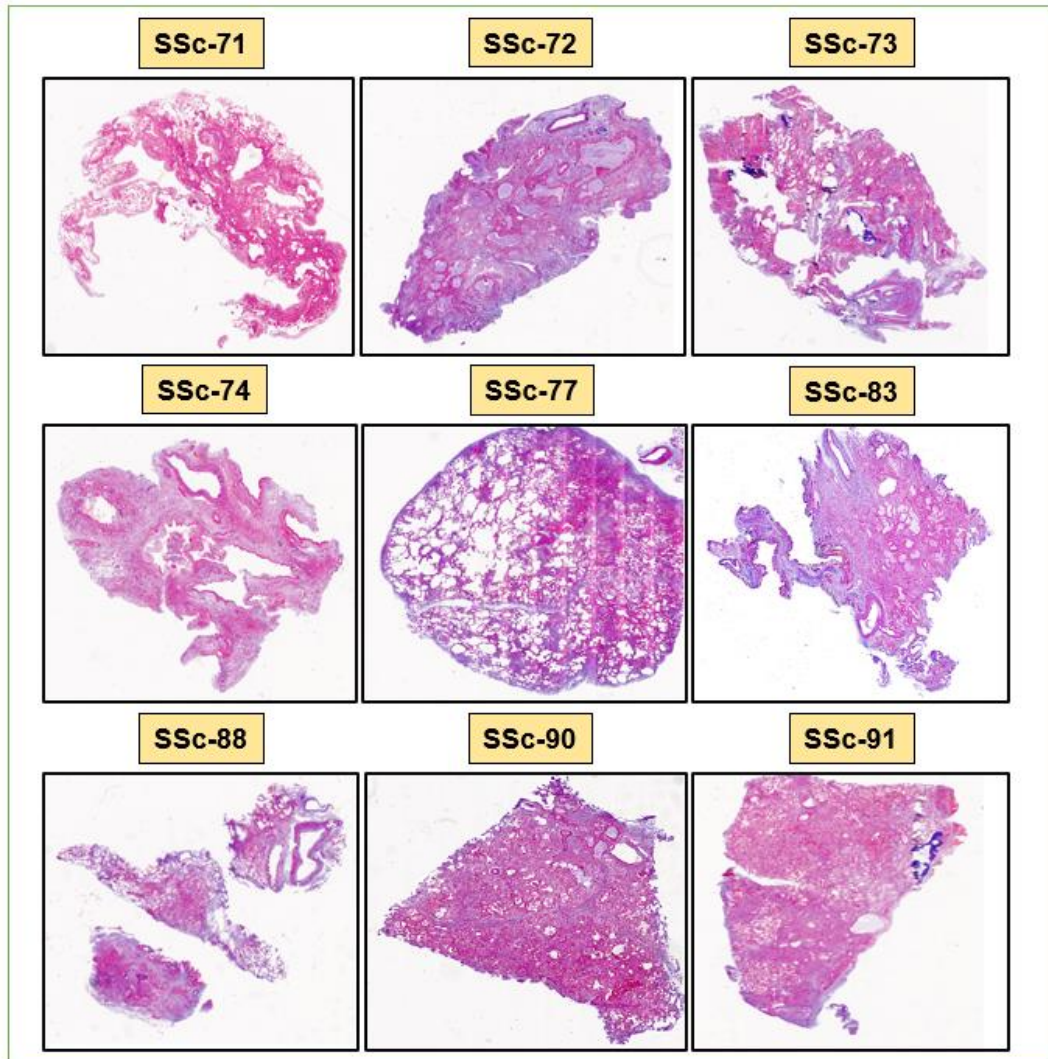


**Figure 3.** Masson's trichrome staining of SSc-ILD lung samples. Masson's trichrome staining reveals with blue color the massive collagen deposition in fibrotic lung, while violet color identifies a cellular infiltrate in the stroma and in the alveoli (20x magnification).

Masson's trichrome staining identified poor collagen deposition (blue color) and a modest infiltrate (violet color) in both stroma and alveoli of lung samples of NLC.

All NLC lung samples were estimated to have a visual fibrosis grading score lower than 3/8 and the mean of automatic semi-quantification of collagen tissue was  $0.27 \pm 0.05$  ( $p < 0.001$  vs SSc-ILD).

Masson's trichrome staining of all NLC samples is reported in Figure 4.

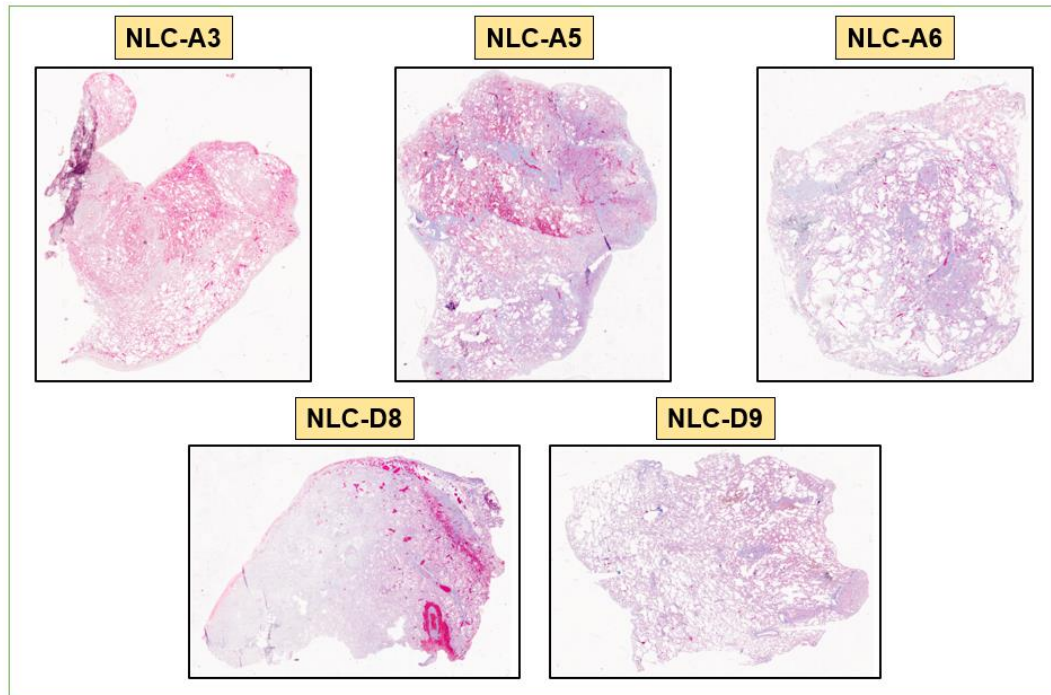


**Figure 4.** Masson's trichrome staining of normal control lung samples. Masson's trichrome staining reveals with blue color a poor collagen deposition, while violet color identifies a little cellular infiltrate in the stroma and in the alveoli (20x magnification).

### **Immunohistochemistry of lung samples**

Immunohistochemistry assay of lungs showed the following expression of surface markers:

- CD68 (pan specific macrophages marker): CD68+ cells were high represented in the stroma and in the alveoli of SSc-ILD patients, significantly more frequent than in NLC ( $p < 0.001$ ).
- CD80 (M1 marker): CD80+ cells were found in the stroma and in alveoli of SSc-ILD patients with overlap with the positivity for CD68+ cells. CD80+ cells were significantly more frequent than in NLC ( $p < 0.05$ ), even if absolute CD80+ cells were significantly less than CD68+ cells in SSc-ILD patients ( $p < 0.001$ ).
- CD86 (M1 marker): CD86+ cells were found virtually absent in the stroma of SSc-ILD patients. CD86+ cells were expressed in the alveolar wall layer facing the air, significantly more frequent than in NLC ( $p < 0.01$ ). In SSc-ILD lungs CD86+ cells were in overlap with CD68+ cells, even if significantly less frequent ( $p < 0.001$ ).
- TLR4 (M1 marker): TLR4+ cells were very diffuse in both stroma and alveoli of SSc-ILD patients, significantly more frequent than in NLC ( $p < 0.0001$ ). In SSc-ILD lungs TLR4+ cells were in overlap with CD68+ cells.
- CD163 (M2 marker): CD163+ cells were very diffuse in both stroma and alveoli of SSc-ILD patients, significantly more frequent than in NLC ( $p < 0.0001$ ). In SSc-ILD lungs CD163+ cells were in overlap with CD68+ cells.
- CD204 (M2 marker): CD204+ cells were very diffuse in both stroma and alveoli of SSc-ILD patients, significantly more frequent than in

NLC ( $p < 0.0001$ ). In SSc-ILD lungs CD204+ cells were in overlap with CD68+ cells.

- CD206 (M2 marker): CD206+ cells are very diffuse in both stroma and alveoli of SSc-ILD patients, significantly more frequent than in NLC ( $p < 0.0001$ ). In SSc-ILD lungs CD206+ cells were in overlap with CD68+ cells.

Example of immunohistochemistry assays performed in SSc-ILD lungs are reported in Figures 5, 6 and 7 (40x magnification), while immunohistochemistry of a NLC is depicted in Figures 8, 9 and 10 (40x magnification).

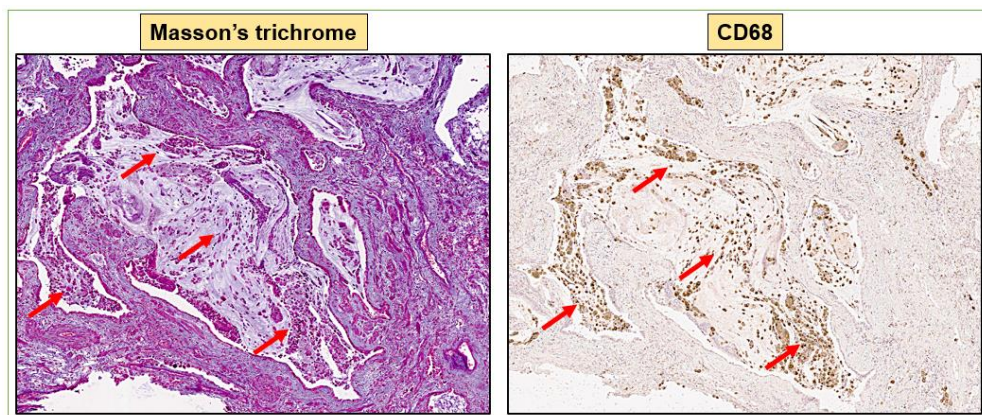


**Figure 5.** Immunohistochemistry of SSc-lung (SSc-83 sample), focusing on Masson's trichrome staining and CD68 positivity. There is a high cell infiltration in the alveoli, expressing CD68 positivity. Red arrows indicate areas rich of cells (violet color for Masson's trichrome and dark color for CD68) (40x magnification).

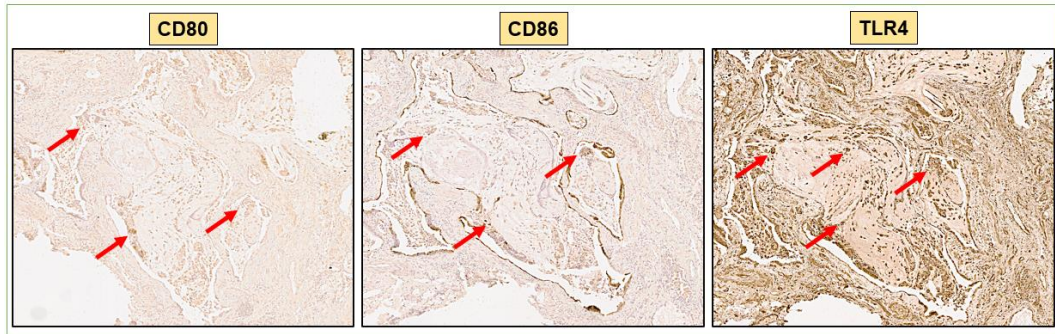


**Figure 6.** Immunohistochemistry of SSc-lung (SSc-83 sample), focusing on M1 markers (CD80, CD86, TLR4) positivity. There is a low expression of CD80 and/or CD86 positive cells, while TLR4 positive cells are frequently found. Red arrows indicate areas positive for each M1 marker (40x magnification).

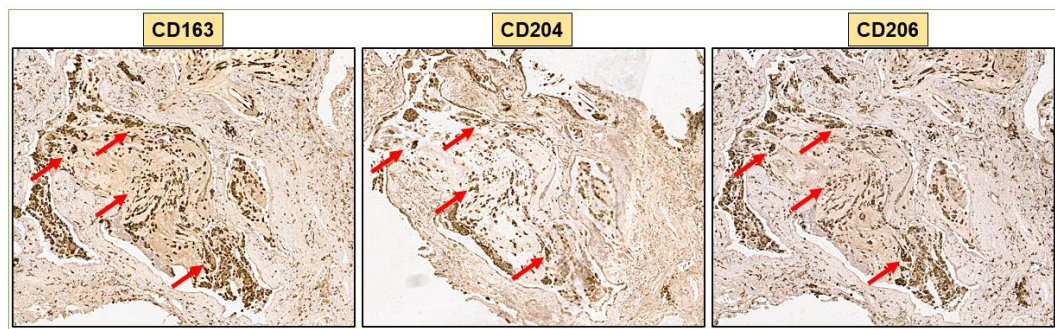


**Figure 7.** Immunohistochemistry of SSc-lung (SSc-83 sample), focusing on M2 markers (CD163, CD204, CD206) positivity. There is a high expression of CD163, CD204 and CD206 positive cells. Red arrows indicate areas positive for each M2 marker (40x magnification).

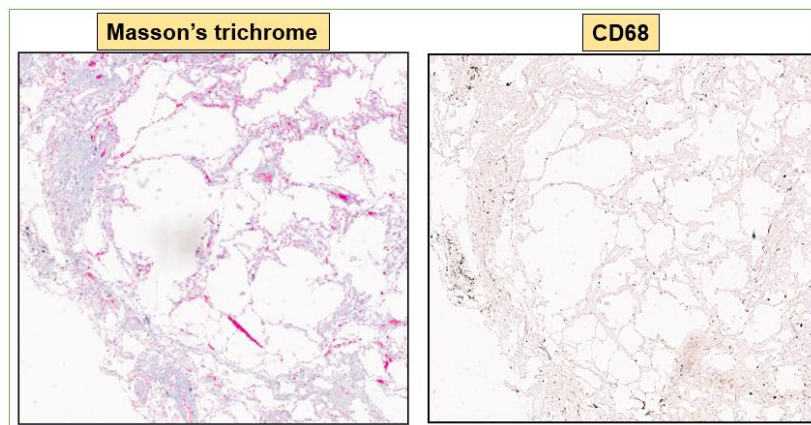


**Figure 8.** Immunohistochemistry of a normal lung control (NLC-A6 sample), focusing on Masson's trichrome staining and CD68 positivity. There are poor collagen deposition and very low cell infiltration in the alveoli. CD68 positive cells are virtually absent (40x magnification).

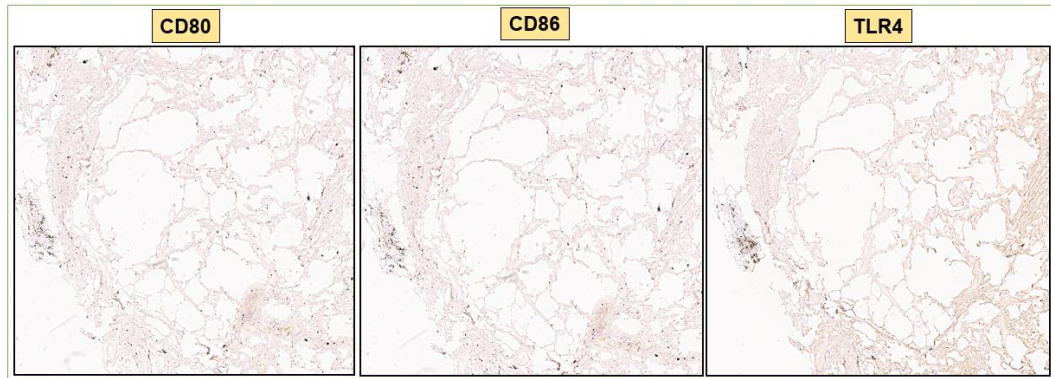


**Figure 9.** Immunohistochemistry of a normal lung control (NLC-A6 sample), focusing on M1 markers (CD80, CD86, TLR4). CD80, CD86 and TLR4 positive cells are virtually absent (40x magnification).

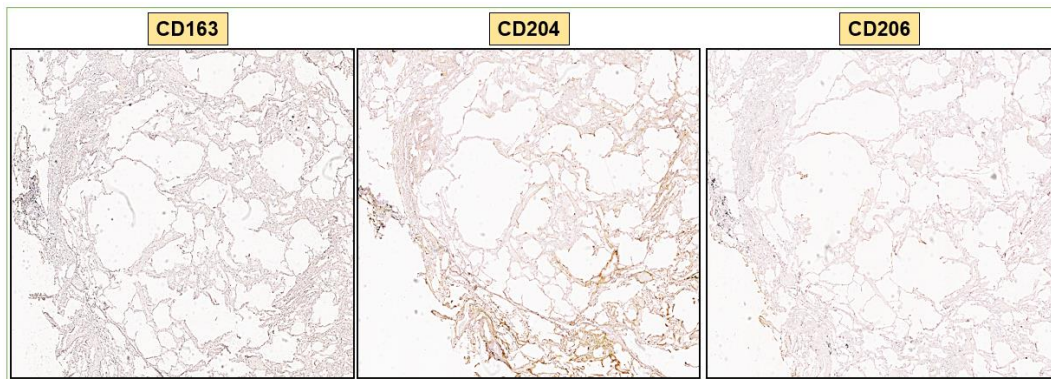


**Figure 10.** Immunohistochemistry of a normal lung control (NLC-A6 sample), focusing on M2 markers (CD163, CD204, CD206). CD163, CD204 and CD206 positive cells are virtually absent (40x magnification).

The summary of the positivity for the surface markers examined in all SSc-ILD lung samples is represented in Figure 11. In the same areas there were a significant overlap between CD68+, TLR4+, CD163+, CD204+ and CD206+ cells (TLR4+M2 macrophages), while CD80+ and CD86+ cells were significantly less represented.

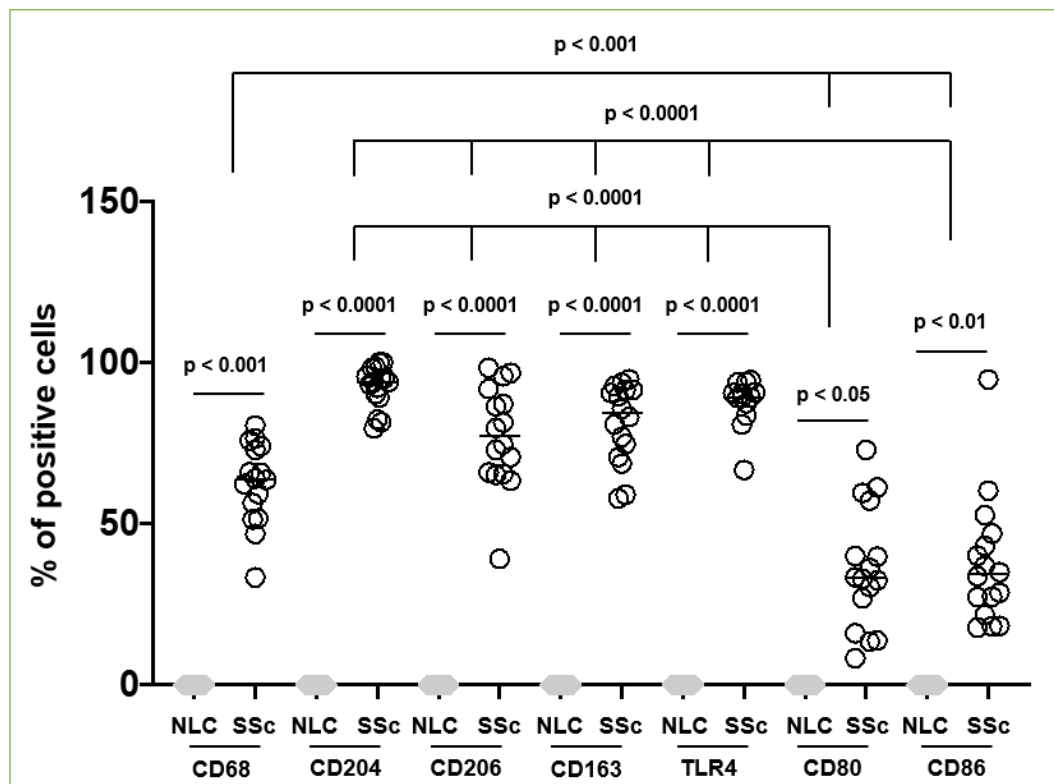


**Figure 11.** Percentage of positivity of surface markers analyzed out of the total cells observed in the SSc-ILD lung samples versus normal lung controls (NLC). Three-quarters of the cells belong to macrophage lineage (CD68) and TLR4 (M1 marker), CD163 (M2 marker), CD204 (M2 marker) and CD206 (M2 marker) were found in the same areas. CD80 (M1 marker) and CD86 (M1 marker) positive cells were significantly less expressed than M2 markers.

## SSc patients and flow cytometry of monocytes

39 consecutive SSc patients (35 females, 4 males, mean age  $62 \pm 16$  years) and 15 HCs (13 females, 2 males,  $58 \pm 10$  years) were recruited for flow cytometry analysis of circulating monocytes. Demographic data of SSc patients are resumed in Table II.

	SSc patients (n=39)
Age (years, mean $\pm$ SD)	$62 \pm 16$
Gender (Female/Male)	35/4
Ethnicity (Caucasian/Afro-American)	38/1
Smokers/Non-smokers	2/37
SSc-ILD (yes/no)	24/15
Anti-topoisomerase I (anti-Scl-70) positivity (yes/no)	17/22
FVC (reference percentage, mean $\pm$ SD)	$89 \pm 32$
DLCO/VA (reference percentage, mean $\pm$ SD)	$75 \pm 20$
Immunosuppressive drugs (mycophenolate mofetil/cyclophosphamide/rituximab)	14/6/6
Antifibrotic drugs (nintedanib/pirfenidone)	3/0

**Table II.** Demographic data of SSc patients and respiratory parameters at time of blood sample. DLCO = Diffusion Lung Carbon Monoxide; FVC = Forced Vital Capacity; ILD = Interstitial Lung Disease; SD = Standard Deviation; SSc = Systemic Sclerosis; VA = Alveolar Volume.

Preliminary results confirmed the significantly higher percentage of circulating monocytes showing M2 surface markers compared to HCs ( $p < 0.001$ ) (Figure 2).

A first analysis was performed dividing SSc patients in two subgroups, according to the presence in the serum of anti-Scl-70 autoantibodies: anti-Scl-70 positive (n=17) and anti-Scl-70 negative (n=22) patients (Table III).

Peripheral Cell phenotype	Anti-Scl-70 + (n=17)	Anti-Scl-70 - (n=22)	P values
CD163+CD204+CD206+	0.5 ± 0.39	0.35 ± 0.17	<0.05
CD80-TLR4-CD163+CD204+CD206+	0.29 ± 0.26	0.18 ± 0.09	<0.05
CD80-TLR4+CD163+CD204+CD206+	0.08 ± 0.07	0.04 ± 0.03	<0.05
CD14+CD80-TLR4-CD163+CD204+CD206+	0.22 ± 0.21	0.12 ± 0.07	<0.01
CD14+CD16+CD80-TLR4+CD163+CD204+CD206+	0.03 ± 0.03	0.02 ± 0.01	<0.05
CD14+CD16+TLR4+CD163+CD204+CD206+	0.05 ± 0.04	0.03 ± 0.02	<0.05
SLAN-CD1c-CD80-TLR4-CD163+CD204+CD206+	0.05 ± 0.04	0.03 ± 0.02	<0.05
SLAN-CD1c-CD80-TLR4+CD163+CD204+CD206+	0.04 ± 0.05	0.02 ± 0.02	0.05

**Table III.** Significant differences observed in the distribution of percentages of circulating cells expressing the monocyte/macrophage markers between SSc patients positive or negative for anti-Scl-70 autoantibodies. Values are expressed as means ± standard deviations of cells percentages.

Of note, the percentage of SLAN-CD1c-CD80-TLR4+CD163+CD204+CD206+ cells (TLR4<sup>+</sup>M2 monocytes) and SLAN-CD1c-CD80-TLR4-CD163+CD204+CD206+ cells (M2 monocytes) were significantly higher in anti-Scl-70 positive SSc patients compared with anti-Scl-70 negative SSc patients (p = 0.05 and p < 0.05, respectively) (Figures 12 and 13).

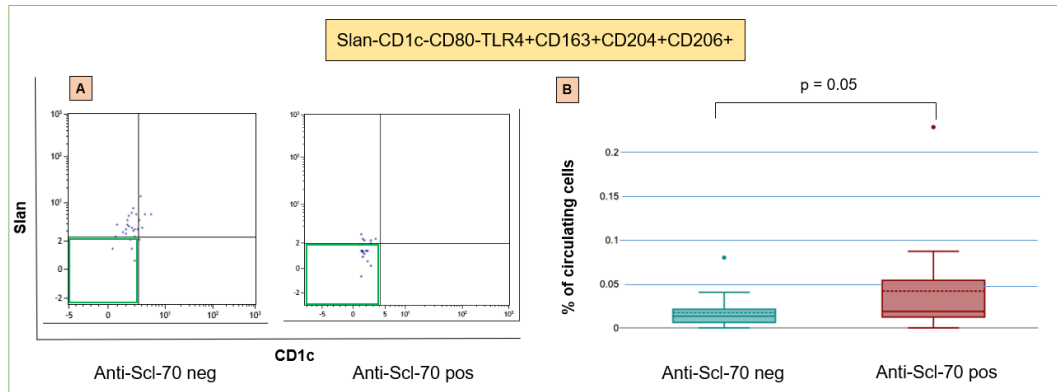


**Figure 12.** Flow cytometry plot (A) of Slan-CD1c-CD80-TLR4+CD163+CD204+CD206+ cells in anti-Scl-70 negative/positive systemic sclerosis patients and related differences in the percentage of circulating cells (B).

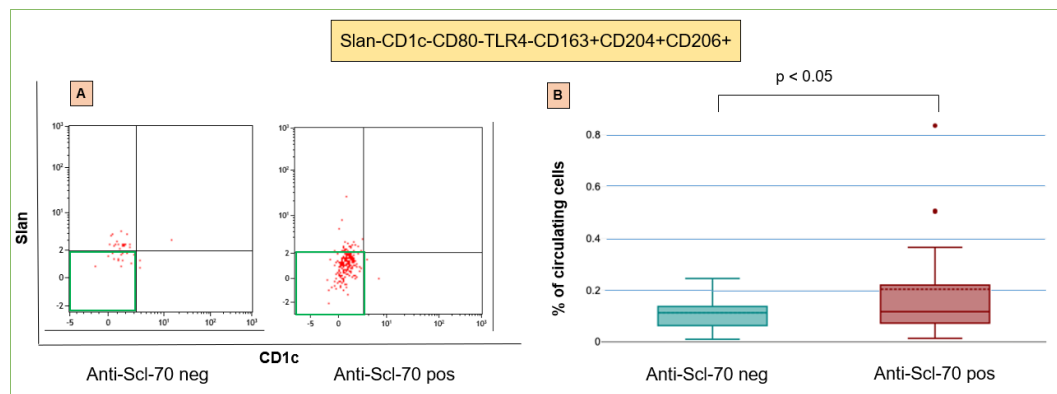


**Figure 13.** Flow cytometry plot (A) of Slan-CD1c-CD80-TLR4-CD163+CD204+CD206+ cells in anti-Scl-70 negative/positive systemic sclerosis patients and related differences in the percentage of circulating cells (B).

A second analysis was performed dividing SSc patients in two subgroups, according to the presence of SSc-ILD: SSc-ILD positive (n=24) and SSc-ILD negative (n=15) (Table IV).

Peripheral Cell phenotype	SSc-ILD + (n=24)	SSc-ILD - (n=15)	P values
SLAN-CD1c-CD80-TLR4-CD163+CD204+CD206+	0.17 ± 0.19	0.13 ± 0.08	0.05
SLAN-CD1c-CD80-TLR4+CD163+CD204+CD206+	0.01 ± 0.01	0 ± 0	< 0.05

**Table IV.** Significant differences observed in the distribution of percentages of circulating cells expressing the monocyte/macrophage markers between SSc patients positive or negative for interstitial lung disease (ILD). Values are expressed as means ± standard deviations of cells percentages.

Of note, the percentage of SLAN-CD1c-CD80-TLR4+CD163+CD204+CD206+ cells (TLR4<sup>+</sup>M2 monocytes) and SLAN-CD1c-CD80-TLR4-CD163+CD204+CD206+ cells (M2 monocytes) were significantly higher in SSc-ILD positive patients compared with SSc-ILD negative patients ( $p < 0.05$  and  $p = 0.05$ , respectively) (Figures 14 and 15).

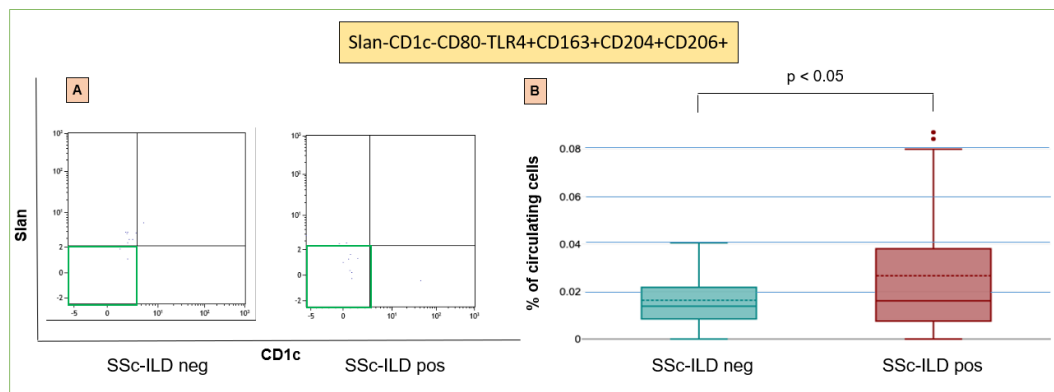


**Figure 14.** Flow cytometry plot (A) of Slan-CD1c-CD80-TLR4+CD163+CD204+CD206+ cells in systemic sclerosis patients with or without interstitial lung disease and related differences in the percentage of circulating cells (B).

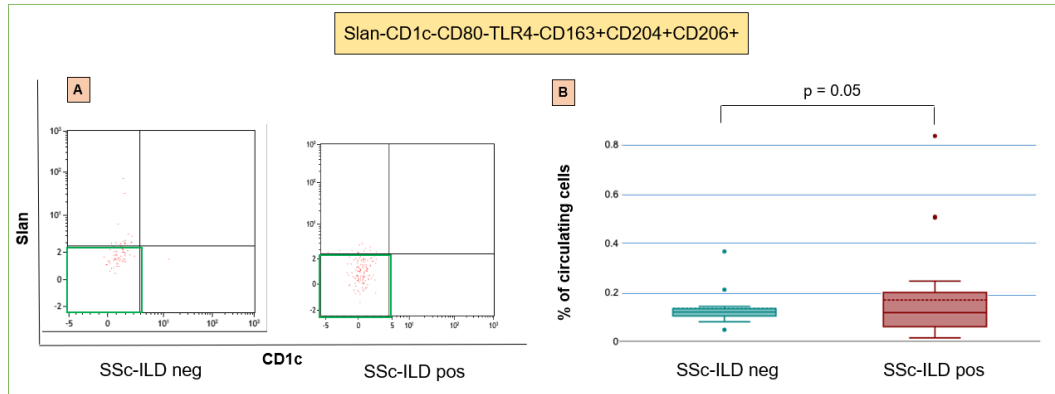


**Figure 15.** Flow cytometry plot (A) of Slan-CD1c-CD80-TLR4-CD163+CD204+CD206+ cells in systemic sclerosis patients with or without interstitial lung disease and related differences in the percentage of circulating cells (B).

## DISCUSSION

Monocyte/macrophage polarization is a dynamic process, influenced by cellular and cytokine environment, and M1/M2 paradigm does not fully reflect the complexity of the biological process in course of autoimmune diseases [54].

A recent study from our Laboratory has demonstrated that circulating monocytes from SSc patients simultaneously express M1 (CD80, CD86, TLR4) and M2 (CD163, CD204, CD206) markers to a greater extent than HCs [38]. Furthermore, this “hybrid” circulating monocyte population (M1/M2) was found to be significantly correlated with the presence of SSc-ILD [39].

For this reason, the current study aimed to investigate the distribution of the M1, M2 or M1/M2 macrophage populations in SSc lung tissue, one of the organs most affected during SSc progression.

Interestingly, the study demonstrated the presence of a rich infiltrate of macrophages (CD68+ cells) in the alveoli and in the fibrotic areas of SSc-ILD patients, compared with NLC of non-SSc patients.

There was a significant prevalence in the lungs of the M2 phenotype, in agreement with previous studies in scleroderma skin, where CD68+CD163+CD204+ cells were significantly more represented than in HCs [55].

In addition, to the presence of the scavenger receptors CD163 and CD204, the current study highlighted the presence of the CD206 receptor

in the same areas of CD68+ cells, further characterizing the increased M2 polarization of scleroderma lung macrophages [56].

Moreover, TLR4 (M1 marker) was significantly co-express in M2 macrophages positive areas of the lung, suggesting for the first time the presence of TLR4<sup>+</sup>M2 macrophages as a significative population in SSc-ILD lungs.

Of note, TLR4 signaling pathway is a driver of fibrosis in scleroderma skin and lung [57]. TLR4 is classically recognized as the receptor for lipopolysaccharide, but also endogenous ligands of “damage-associated molecular patterns” (DAMPs) can activate it [58].

The most frequent DAMPs in course of SSc have been identified in some components of the ECM, such as tenascin C and fibronectin-EDA [58].

Once recognized by TLR4, these molecules activate a signaling pathway that includes the accessory protein MD2 and ends with the differentiation of tissue fibroblasts into myofibroblasts, further supporting the pulmonary fibrotic process [59].

The presence of TLR4<sup>+</sup>M2 macrophages in SSc-ILD samples analyzed does not seem to be influenced by immunosuppressive therapies of patients awaiting lung transplantation [60].

In fact, SSc patients were treated with variable combination of mycophenolate mofetil, calcineurin inhibitors (cyclosporine A and tacrolimus), basiliximab (anti-CD25) and alemtuzumab (anti-CD52), reflecting on-label and off-label therapies for SSc-ILD available in USA before 2010.

Clearly, new antifibrotic and immunomodulatory therapies for SSc-ILD might also interfere with lung macrophages polarization and is matter of our further research.

Nintedanib is a tyrosine kinase inhibitor, licensed for the treatment of SSc-ILD [61]. In the fos-related antigen-2 (Fra2) mouse model of SSc, nintedanib significantly reduces M2 polarization, also reducing the total number of M2 macrophages [62].

Moreover, nintedanib partially blocks the expression of M2 markers, including CD206, in primary cultures of human monocyte-derived macrophages controlled by human recombinant colony-stimulating factor 1 [63].

The effects of nintedanib on M2 macrophage polarization further support the overall antifibrotic effect, hindering the transition of fibrocytes into myofibroblasts as already reported in our studies [64,65].

Pirfenidone is a drug licensed for the treatment of idiopathic pulmonary fibrosis, currently under investigation for SSc-ILD [66]. Pirfenidone attenuates fibroblast proliferation, production of proteins and cytokines associated to fibrosis and the increase in biosynthesis and accumulation of ECM in response to TGF- $\beta$  [67]. Of note, in mouse models, pirfenidone reduces M2 polarization, downregulating transcription factor NF- $\kappa$ B [68,69].

Janus kinase inhibitors are a class of synthetic molecule capable of blocking the activation of janus kinases (JAK1, JAK2, JAK3) and tyrosine kinase 2 (Tyk2) [70]. These drugs are not marketed for the treatment of

SSc but *in vitro* studies on monocyte-derived macrophages from healthy donors and on lung biopsies of hypochlorous acid mouse model of SSc-ILD demonstrated a significant effect in downregulating M2 polarization [71].

Current on-label and off-label pharmacological therapies for SSc-ILD are partially satisfactory and the search for precision therapy is a more urgent need than ever [72].

The here reported identification of TLR4<sup>+</sup>M2 macrophages can represent an aid in the design of increasingly specific drugs.

Of note, TLR4<sup>+</sup>M2 markers have been detected also in peripheral monocytes of SSc patients, together with TLR4<sup>-</sup>M2 markers, and were significantly higher in anti-Scl-70 positive SSc-patients than anti-Scl-70 negative and in SSc-ILD positive patients than SSc-ILD negative.

Peripheral SSc-monocyte populations have been characterized with as much precision as possible, excluding CD1c<sup>+</sup> and Slan<sup>+</sup> cells [73].

CD1c is a marker of dendritic cells type II and identifies a subset that can be CD14<sup>+</sup>, expressing also monocyte associated genes (i.e., CD115, MAFB, S100A8/9) [74].

Slan<sup>+</sup> monocytes have been observed to contribute to the immune pathogenesis of different inflammatory and autoimmune diseases [75].

Slan<sup>+</sup> monocytes can be precursors of both dendritic cells and tissue macrophages that eliminate tumor cells [76].

So, data collected from lung samples and peripheral blood seems of great importance since TLR4<sup>+</sup>M2 monocytes/macrophages seem associated

with radiographic ILD, histological fibrosis and anti-Scl-70 positivity, suggesting a possible role as a biomarker of SSc-ILD.

At last, the study has some limitations. First, a single immunostaining was performed for each lung tissue section, without conferring absolute certainty that the positive macrophage markers are expressed by the same cells. An analysis with multiplex immunoassays is mandatory and already planned to confirm the presence of cells co-expressing M1/M2 markers in the fibrotic areas of the lung [77].

Furthermore, once the presence of TLR4<sup>+</sup>M2 macrophages has been confirmed in SSc-ILD samples, cytokine expression of these cells will be analyzed/characterized with immunofluorescence, ELISA and/or real time PCR in our Laboratories.

In fact, further studies should focus more precisely on classifying macrophage populations to shed a light on direct lineages of TLR4<sup>+</sup>M2 macrophages, deriving from lung resident macrophages or peripheral blood monocytes (i.e., transcriptomic analysis) [78].

A more extensive sampling organ collection, including skin and gastrointestinal tissues will allow to evaluate further correlations, between hybrid monocyte/macrophage populations and organ damage [79,80].

In conclusion, in this study monocytes/macrophage specific phenotypes seems to characterize in lung as well as in blood samples of patients with SSc-ILD generating original results.

## REFERENCES

1. Cutolo M, Soldano S, Smith V. Pathophysiology of systemic sclerosis: current understanding and new insights. *Expert Rev Clin Immunol*. 2019;15(7):753-764.
2. Volkman ER, Andréasson K, Smith V. Systemic sclerosis. *Lancet*. 2023;401(10373):304-318.
3. Haque A, Hughes M. Raynaud's phenomenon. *Clin Med (Lond)*. 2020;20(6):580-587.
4. Mostmans Y, Cutolo M, Giddelo C, et al. The role of endothelial cells in the vasculopathy of systemic sclerosis: A systematic review. *Autoimmun Rev*. 2017;16(8):774-786.
5. Kawaguchi Y, Kuwana M. Pathogenesis of vasculopathy in systemic sclerosis and its contribution to fibrosis. *Curr Opin Rheumatol*. 2023;35(6):309-316.
6. Fang D, Chen B, Lescoat A, et al. Immune cell dysregulation as a mediator of fibrosis in systemic sclerosis. *Nat Rev Rheumatol*. 2022;18(12):683-693.
7. Cutolo M, Smith V. Detection of microvascular changes in systemic sclerosis and other rheumatic diseases. *Nat Rev Rheumatol*. 2021;17(11):665-677.
8. Smith V, Ickinger C, Hysa E, et al. Nailfold capillaroscopy. *Best Pract Res Clin Rheumatol*. 2023;101849.
9. Hysa E, Campitiello R, Sammorì S, et al. Specific Autoantibodies and Microvascular Damage Progression Assessed by Nailfold Videocapillaroscopy in Systemic Sclerosis: Are There Peculiar Associations? An Update. *Antibodies (Basel)*. 2023;12(1):3.
10. Graßhoff H, Fourlakis K, Comdühr S, et al. Autoantibodies as Biomarker and Therapeutic Target in Systemic Sclerosis. *Biomedicines*. 2022;10(9):2150.

11. Perelas A, Silver RM, Arrossi AV, et al. Systemic sclerosis-associated interstitial lung disease. *Lancet Respir Med.* 2020;8(3):304-320
12. Haque A, Kiely DG, Kovacs G, et al. Pulmonary hypertension phenotypes in patients with systemic sclerosis. *Eur Respir Rev.* 2021;30(161):210053.
13. Moysidou GS, Dara A, Arvanitaki A, et al. Understanding and managing cardiac involvement in systemic sclerosis. *Expert Rev Clin Immunol.* 2023;19(3):293-304.
14. Scheen M, Dominati A, Olivier V, et al. Renal involvement in systemic sclerosis. *Autoimmun Rev.* 2023;22(6):103330.
15. Volkmann ER, McMahan Z. Gastrointestinal involvement in systemic sclerosis: pathogenesis, assessment and treatment. *Curr Opin Rheumatol.* 2022;34(6):328-336.
16. Thietart S, Louati K, Gatifosse M, et al. Overview of osteo-articular involvement in systemic sclerosis: Specific risk factors, clinico-sonographic evaluation, and comparison with healthy women from the French OFELY cohort. *Best Pract Res Clin Rheumatol.* 2018;32(4):591-604.
17. Chaigne B, Léonard-Louis S, Mouthon L. Systemic sclerosis associated myopathy. *Autoimmun Rev.* 2023;22(2):103261.
18. van den Hoogen F, Khanna D, Fransen J, et al. 2013 classification criteria for systemic sclerosis: an American college of rheumatology/European league against rheumatism collaborative initiative. *Ann Rheum Dis.* 2013;72(11):1747-55.
19. Khanna D, Tashkin DP, Denton CP, et al. Etiology, Risk Factors, and Biomarkers in Systemic Sclerosis with Interstitial Lung Disease. *Am J Respir Crit Care Med.* 2020;201(6):650-660.
20. Sarrand J, Soyfoo MS. Involvement of Epithelial-Mesenchymal Transition (EMT) in Autoimmune Diseases. *Int J Mol Sci.* 2023;24(19):14481.

21. Liakouli V, Ciancio A, Del Galdo F, et al. Systemic sclerosis interstitial lung disease: unmet needs and potential solutions. *Nat Rev Rheumatol*. 2024;20(1):21-32.
22. Cottin V, Brown KK. Interstitial lung disease associated with systemic sclerosis (SSc-ILD). *Respir Res*. 2019;20(1):13.
23. Jacquerie P, André B, De Seny D, et al. Reproducibility of pulmonary function tests in patients with systemic sclerosis. *Sci Rep*. 2023;13(1):18960.
24. Khanna D, Distler O, Cottin V, et al. Diagnosis and monitoring of systemic sclerosis-associated interstitial lung disease using high-resolution computed tomography. *J Scleroderma Relat Disord*. 2022;7(3):168-178.
25. Cottin V, Brown KK. Interstitial lung disease associated with systemic sclerosis (SSc-ILD). *Respir Res*. 2019;20(1):13.
26. Poudel DR, Jayakumar D, Danve A, et al. Determinants of mortality in systemic sclerosis: a focused review. *Rheumatol Int*. 2018;38(10):1847-1858.
27. Raghu G, Remy-Jardin M, Richeldi L, et al. Idiopathic Pulmonary Fibrosis (an Update) and Progressive Pulmonary Fibrosis in Adults: An Official ATS/ERS/JRS/ALAT Clinical Practice Guideline. *Am J Respir Crit Care Med*. 2022;205(9):e18-e47.
28. Bonhomme O, André B, Gester F, et al. Biomarkers in systemic sclerosis-associated interstitial lung disease: review of the literature. *Rheumatology (Oxford)*. 2019;58(9):1534-1546.
29. Smith V, Vanhaecke A, Guerra MG, et al. May capillaroscopy be a candidate tool in future algorithms for SSC-ILD: Are we looking for the holy grail? A systematic review. *Autoimmun Rev*. 2020;19(9):102619.
30. Rahaghi FF, Hsu VM, Kaner RJ, et al. Expert consensus on the management of systemic sclerosis-associated interstitial lung disease. *Respir Res*. 2023;24(1):6.

31. Kawakami A, Iwamoto N, Fujio K. Editorial: The role of monocytes/macrophages in autoimmunity and autoinflammation. *Front Immunol.* 2022;13:1093430.
32. Mitchell AJ, Roediger B, Weninger W. Monocyte homeostasis and the plasticity of inflammatory monocytes. *Cell Immunol.* 2014;291(1-2):22-31.
33. Oishi Y, Manabe I. Macrophages in inflammation, repair and regeneration. *Int Immunol.* 2018;30(11):511-528.
34. Huang X, Li Y, Fu M, et al. Polarizing Macrophages In Vitro. *Methods Mol Biol.* 2018;1784:119-126.
35. Higashi-Kuwata N, Jinnin M, Makino T, et al. Characterization of monocyte/macrophage subsets in the skin and peripheral blood derived from patients with systemic sclerosis. *Arthritis Res Ther.* 2010;12(4):R128.
36. Mathai SK, Gulati M, Peng X, et al. Circulating monocytes from systemic sclerosis patients with interstitial lung disease show an enhanced profibrotic phenotype. *Lab Invest.* 2010;90(6):812-23.
37. Rudnik M, Hukara A, Kocherova I, et al. Elevated Fibronectin Levels in Profibrotic CD14<sup>+</sup> Monocytes and CD14<sup>+</sup> Macrophages in Systemic Sclerosis. *Front Immunol.* 2021;12:642891.
38. Soldano S, Trombetta AC, Contini P, et al. Increase in circulating cells coexpressing M1 and M2 macrophage surface markers in patients with systemic sclerosis. *Ann Rheum Dis.* 2018;77(12):1842-1845.
39. Trombetta AC, Soldano S, Contini P, et al. A circulating cell population showing both M1 and M2 monocyte/macrophage surface markers characterizes systemic sclerosis patients with lung involvement. *Respir Res.* 2018;19(1):186.
40. Mattoo H, Bangari DS, Cummings S, et al. Molecular Features and Stages of Pulmonary Fibrosis Driven by Type 2 Inflammation. *Am J Respir Cell Mol Biol.* 2023;69(4):404-421.

41. Valenzi E, Bulik M, Tabib T, et al. Single-cell analysis reveals fibroblast heterogeneity and myofibroblasts in systemic sclerosis-associated interstitial lung disease. *Ann Rheum Dis.* 2019;78(10):1379-1387.
42. Valenzi E, Tabib T, Papazoglou A, et al. Disparate Interferon Signaling and Shared Aberrant Basaloid Cells in Single-Cell Profiling of Idiopathic Pulmonary Fibrosis and Systemic Sclerosis-Associated Interstitial Lung Disease. *Front Immunol.* 2021;12:595811.
43. Papazoglou A, Huang M, Bulik M, et al. Epigenetic Regulation of Profibrotic Macrophages in Systemic Sclerosis-Associated Interstitial Lung Disease. *Arthritis Rheumatol.* 2022;74(12):2003-2014.
44. Christmann RB, Sampaio-Barros P, Stifano G, et al. Association of Interferon- and transforming growth factor  $\beta$ -regulated genes and macrophage activation with systemic sclerosis-related progressive lung fibrosis. *Arthritis Rheumatol.* 2014;66(3):714-25.
45. Pechkovsky DV, Prasse A, Kollert F, et al. Alternatively activated alveolar macrophages in pulmonary fibrosis-mediator production and intracellular signal transduction. *Clin Immunol.* 2010;137(1):89-101.
46. Al-Adwi Y, Westra J, van Goor H, et al. Macrophages as determinants and regulators of fibrosis in systemic sclerosis. *Rheumatology (Oxford).* 2023;62(2):535-545.
47. Bhandari R, Ball MS, Martyanov V, et al. Profibrotic Activation of Human Macrophages in Systemic Sclerosis. *Arthritis Rheumatol.* 2020;72(7):1160-1169.
48. Lescoat A, Lecreur V, Varga J. Contribution of monocytes and macrophages to the pathogenesis of systemic sclerosis: recent insights and therapeutic implications. *Curr Opin Rheumatol.* 2021;33(6):463-470.

49. Verma, P., Bale, S., Varga, J. et al. Molecular Mechanisms Underlying Systemic Sclerosis–Associated Interstitial Lung Disease and Idiopathic Pulmonary Fibrosis: an Update. *Curr Treat Options in Rheum.* 2023;9:221-235.
50. Ashcroft T, Simpson JM, Timbrell V. Simple method of estimating severity of pulmonary fibrosis on a numerical scale. *J Clin Pathol.* 1988;41(4):467-70.
51. Stritt M, Stalder AK, Vezzali E. Orbit Image Analysis: An open-source whole slide image analysis tool. *PLoS Comput Biol.* 2020;16(2):e1007313.
52. Venè R, Costa D, Augugliaro R, et al. Evaluation of Glycosylated PTGS2 in Colorectal Cancer for NSAIDS-Based Adjuvant Therapy. *Cells.* 2020;9(3):683.
53. Arroz M, Came N, Lin P, et al. Consensus guidelines on plasma cell myeloma minimal residual disease analysis and reporting. *Cytometry B Clin Cytom.* 2016;90(1):31-9.
54. Toledo DM, Pioli PA. Macrophages in Systemic Sclerosis: Novel Insights and Therapeutic Implications. *Curr Rheumatol Rep.* 2019;21(7):31.
55. Higashi-Kuwata N, Makino T, Inoue Y, et al. Alternatively activated macrophages (M2 macrophages) in the skin of patient with localized scleroderma. *Exp Dermatol.* 2009;18(8):727-9.
56. Hu M, Yao Z, Xu L, et al. M2 macrophage polarization in systemic sclerosis fibrosis: pathogenic mechanisms and therapeutic effects. *Heliyon.* 2023;9(5):e16206.
57. Bhattacharyya S, Kelley K, Melichian DS, et al. Toll-like receptor 4 signaling augments transforming growth factor- $\beta$  responses: a novel mechanism for maintaining and amplifying fibrosis in scleroderma. *Am J Pathol.* 2013;182(1):192-205.
58. Bhattacharyya S, Varga J. Endogenous ligands of TLR4 promote unresolving tissue fibrosis: Implications for systemic sclerosis and its targeted therapy. *Immunol Lett.* 2018;195:9-17.

59. O'Reilly S, van Laar JM. Targeting the TLR4-MD2 axis in systemic sclerosis. *Nat Rev Rheumatol.* 2018;14(10):564-566.
60. Mendoza FA, Allawh T, Jimenez SA. Pharmacological treatment of systemic sclerosis-associated interstitial lung disease: an updated review and current approach to patient care. *Clin Exp Rheumatol.* 2023;41(8):1704-1712.
61. Distler O, Highland KB, Gahlemann M, et al. Nintedanib for Systemic Sclerosis-Associated Interstitial Lung Disease. *N Engl J Med.* 2019;380(26):2518-2528.
62. Huang J, Maier C, Zhang Y, et al. Nintedanib inhibits macrophage activation and ameliorates vascular and fibrotic manifestations in the Fra2 mouse model of systemic sclerosis. *Ann Rheum Dis.* 2017;76(11):1941-1948.
63. Bellamri N, Morzadec C, Joannes A, et al. Alteration of human macrophage phenotypes by the anti-fibrotic drug nintedanib. *Int Immunopharmacol.* 2019;72:112-123.
64. Cutolo M, Gotelli E, Montagna P, et al. Nintedanib downregulates the transition of cultured systemic sclerosis fibrocytes into myofibroblasts and their pro-fibrotic activity. *Arthritis Res Ther.* 2021;23(1):205. Erratum in: *Arthritis Res Ther.* 2023;25(1):134.
65. Soldano S, Smith V, Montagna P, et al. Nintedanib downregulates the profibrotic M2 phenotype in cultured monocyte-derived macrophages obtained from systemic sclerosis patients affected by interstitial lung disease. *Arthritis Res Ther.* 2024;26(1):74.
66. Pope JE, Denton CP, Johnson SR, et al. State-of-the-art evidence in the treatment of systemic sclerosis. *Nat Rev Rheumatol.* 2023;19(4):212-226.

67. Lv Q, Wang J, Xu C, et al. Pirfenidone alleviates pulmonary fibrosis in vitro and in vivo through regulating Wnt/GSK-3 $\beta$ / $\beta$ -catenin and TGF- $\beta$ 1/Smad2/3 signaling pathways. *Mol Med*. 2020;26(1):49.
68. Toda M, Mizuguchi S, Minamiyama Y, et al. Pirfenidone suppresses polarization to M2 phenotype macrophages and the fibrogenic activity of rat lung fibroblasts. *J Clin Biochem Nutr*. 2018;63(1):58-65.
69. Ying H, Fang M, Hang QQ, et al. Pirfenidone modulates macrophage polarization and ameliorates radiation-induced lung fibrosis by inhibiting the TGF- $\beta$ 1/Smad3 pathway. *J Cell Mol Med*. 2021;25(18):8662-8675.
70. Roskoski R Jr. Janus kinase (JAK) inhibitors in the treatment of neoplastic and inflammatory disorders. *Pharmacol Res*. 2022 Sep;183:106362.
71. Lescoat A, Lelong M, Jeljeli M, et al. Combined anti-fibrotic and anti-inflammatory properties of JAK-inhibitors on macrophages in vitro and in vivo: Perspectives for scleroderma-associated interstitial lung disease. *Biochem Pharmacol*. 2020;178:114103.
72. Khedoe P, Marges E, Hiemstra P, et al. Interstitial Lung Disease in Patients With Systemic Sclerosis: Toward Personalized-Medicine-Based Prediction and Drug Screening Models of Systemic Sclerosis-Related Interstitial Lung Disease (SSc-ILD). *Front Immunol*. 2020;11:1990.
73. Schröder M, Melum GR, Landsverk OJ, et al. CD1c-Expression by Monocytes - Implications for the Use of Commercial CD1c+ Dendritic Cell Isolation Kits. *PLoS One*. 2016;11(6):e0157387.
74. Heger L, Hofer TP, Bigley V, et al. Subsets of CD1c<sup>+</sup> DCs: Dendritic Cell Versus Monocyte Lineage. *Front Immunol*. 2020;11:559166.
75. Ahmad F, Döbel T, Schmitz M, et al. Current Concepts on 6-sulfo LacNAc Expressing Monocytes (slanMo). *Front Immunol*. 2019;10:948.

76. Vermi W, Micheletti A, Finotti G, et al. slan<sup>+</sup> Monocytes and Macrophages Mediate CD20-Dependent B-cell Lymphoma Elimination via ADCC and ADCP. *Cancer Res.* 2018;78(13):3544-3559.
77. Harms PW, Frankel TL, Moutafi M, et al. Multiplex Immunohistochemistry and Immunofluorescence: A Practical Update for Pathologists. *Mod Pathol.* 2023;36(7):100197.
78. Mehta BK, Espinoza ME, Hinchcliff M, et al. Molecular "omic" signatures in systemic sclerosis. *Eur J Rheumatol.* 2020;7(Suppl 3):S173-S180.
79. Mohamed ME, Gamal RM, El-Mokhtar MA, et al. Peripheral cells from patients with systemic sclerosis disease co-expressing M1 and M2 monocyte/macrophage surface markers: Relation to the degree of skin involvement. *Hum Immunol.* 2021;82(9):634-639.
80. Peng Y, Zhou M, Yang H, et al. Regulatory Mechanism of M1/M2 Macrophage Polarization in the Development of Autoimmune Diseases. *Mediators Inflamm.* 2023;2023:8821610.